EFFECT OF BEAM LOSSES ON WIRE SCANNER SCINTILLATOR READOUT, HYPOTHESIS AND PRELIMINARY RESULTS

B. Cheymol*, European Spallation Source, Lund, Sweden

Abstract

In an hadron accelerator, the characterization of the beam transverse halo can lead to a better understanding of the beam dynamics and a reduction of the beam losses. Unfortunately the effect of losses on beam instrumentation implies a reduction of the instrument sensitivity due to the background noise.

In this paper, we will discuss the effect of losses on the wire scanner scintillator foreseen for the ESS linac, in particular the different hypothesis for the input will be describes and preliminary results will be present.

INTRODUCTION

In the elliptical sections of the ESS linac [1] the Wire Scanner (WS) station will be equipped with scintillators to measure the hadronic shower created by a thin tungsten wire [2]. One of the main reasons is that above 200 MeV the secondary emission signal is not strong enough to measure directly the current produced in the wire, the signal from a scintillator will be stronger and also cleaner, but this detector will be also sensitive to radiation induced by beam losses. Preliminary simulations have been performed to check this effect and define beam loss limits for the WS operation.

Several beam losses scenario have been simulated with the Monte Carlo (MC) code FLUKA [3] in order to estimate the influence of losses on the beam profile measurement. Note that all the particles distributions presented in this paper are not the results of beam dynamic simulations.

HYPOTHESIS AND INPUT PARAMETERS

Hypothesis

To simplify the problem, we propose to study the effect of various beam losses scenario in a single elliptical period (one elliptical cryomodule followed by one quadrupole doublet). It was assumed, in a first approximation, that the contribution from upstream or downstream losses will be either too low to be detected or easily removed in the data analysis.

A simplified geometry of an elliptical cryomodule has been implemented in the MC code, only the main components have been simulated, all the cryogenic pipe, cable, RF guide have not been implemented in the simulated geometry. Despite the fact that the Medium and High β cavities are slightly different, the geometry is independent of the beam energy, a 5 cells cavity has been chosen for this study, which the one foreseen to be installed in the High β section for beam energy above 570 MeV, the length of the cryomodule is about 6.5 meters. The quadruples consists in a single volume of copper. The author would like to emphasis that no electromagnetic field has been implemented in the simulations.

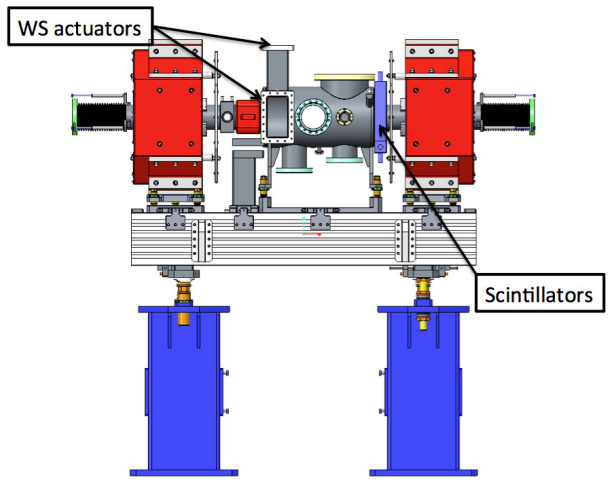

Figure 1: Preliminary design of the elliptical LWU, the length flange to flange is 1920 mm (courtesy of STFC Daresbury Laboratory).

The Linac Warm Unit (LWU) chamber has been simulated (see Fig. 1), the scintillator are attached to this chamber, the detector assembly is shown in Fig. 2. The minimum aperture in the LWU is 100 mm.

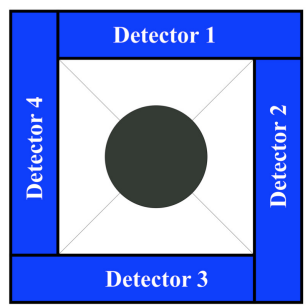

Figure 2: Detector assembly for the ESS WS system.

The scintillator material in these simulations are not the one foreseen to be used for the ESS WS system, in preliminary design phase of the WS detector BGO crystal was the primary candidate for the scintillator and all the simulations presented in this paper have been performed with this type of scintillator. nevertheless, since the geometry is identical, the signal to noise ratio shall be comparable for both versions of the detector.

For this simulations and in a first approximation, the beam sizes of the core were assumed to be constant in the cold linac with $\sigma_x = \sigma_y = 2$ mm. The beam has no energy spread.

* benjamin.cheymol@esss.se

ISBN 978-3-95450-178-6

Beam Distributions for the Simulations

Full beam loss In order to get a overall vision of beam loss effect on scintillators, a series of simulations have been performed with a pencil beam interacting with the beam pipe in the middles of quadrupoles. Simulations have been performed at 2 positions, in the middle of the upstream quadrupole and in the middle of the downstream quadrupole with respect of the detector position (see Fig. 1). The angle of impact was varying from 1 to 250 mrad and the beam energy from 200 to 2000 MeV.

A second series of simulations were done in order to check the effect of unwanted steering of the beam. The beams were created at the beginning of the cell at the center of beam pipe, an angular kick of 6 mrad and 10 mrad was given to the particles in order to have the interaction point of the beam center with the beam pipe in the center of the quadrupole and in the center of the cryomodule. the beam energy was varying from 200 to 2000 MeV. For this cases, only the beam core has been simulated

For all the losses simulated, the beam impacts on the upper quadrant of the beam pipe.

Halo During the operation of the WS system, the background noise will be mainly generated by losses due to particles lost from the beam halo (only the transverse halo has been considered in this study). In order to decrease the time of the MC simulations and have a good statistic, hollow beams have been simulated with a minimum radius of 10 mm. The origin of the beam is set at 100 mm upstream to the cryomodule entrance.

The beam halo distributions are difficult to predict, several distributions have been considered in order to explore a large range of possibilities from a fully unmatched beam to almost perfect matching of the beam to the lattice. The distributions are identical in both planes.

In the worst case scenario, the particles will fill all the geometrical acceptance the cold linac, in a first approximation, the influence of the beam energy on the particle distribution in the phase space has been neglected. In real space, the particles were generated in ring with a minimum radius of 10 mm and a maximum radius of 45 mm with a uniform density , the particles divergence was set to ± 7.5 mrad and to $\sigma_{x'}$=6 mrad, these values corresponds to twice the geometrical acceptance of an elliptical section period, beam energy was scan form 200 MeV to 2000 MeV.

Similar simulations have been performed with different cut in the real space (15 σ and 10 σ of the beam core), with a distribution of the particle divergence equal to ± 6 mrad and ± 4mrad, all distributions have been considered uniform.

Based on the work presented in [4], several beam distributions were generated to simulate intermediate cases between a "fully filamented" beam presented above and an ideal beam "matched" to the structure. Beam sizes were assumed to be independent of the beam energy, as well as the distribution of the halo in the real space, while, in order to simulate the effect of the acceleration, the divergence of the particles decreases with the beam energy. Uniform and gaussian distributions have been simulated, for gaussian distribution we assumed that the halo has an rms of 4 times the rms of the beam core (i.e 8 mm). Several cute has been simulated (20 σ,15 σ and 10 σ of the beam core), and i In the simulations. The beam halo divergence is increased by at least a factor 2 compare to the ideal beam in case of a gaussian distribution, for the flat distribution, the maximum divergence is ≈ 6 times the rms value of the ideal beam divergence. In addition, a smaller divergence has been simulated with an increase of few tens of percent compare to the distributions presented in [4], to simulate an optimal case with reduces losses. The evolutions of the divergence as function of the beam energy is shown in Fig. 3.

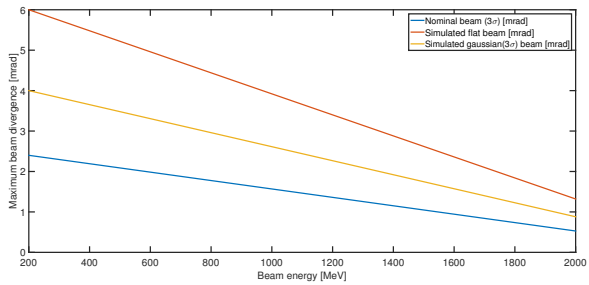

Figure 3: Maximum simulated divergence as function of the beam energy. In the document, the red curve is refereed to "flat", the yellow curve to "gauss high" and the blue one to "gauss low".

The parameters of the various simulated distribution are summarized in Tab. 1 and Tab. 2, in the next sections of this paper, the distribution will be referenced by the name presented in the table.

Table 1: Summary of the beam distribution simulated when they are independent of the beam energy. Extension in real space are given in term of σ of the beam core

	Extension	
Name	real space	divergence
"fil. uniform"	22.5σ uniform	± 7.5 mrad uniform
"fil. gauss"	22.5σ uniform	$\sigma_{x'}$ (1 rms) = 6 mrad
"15 6"	15σ uniform	± 6 mrad uniform
"15 4"	15σ uniform	± 4mrad uniform
"10 6"	10σ uniform	± 6 mrad uniform
"10 4"	10σ uniform	± 4mrad uniform

As example, the particles distribution in the phase space for two the extreme cases are shown in Figs. 4 and 5.

PRELIMINARY RESULTS

Full Beam Loss

As shown in Fig. 6 to Fig. 8, the energy deposited in the detector 1 is strongly dependent of the losses angle, and less on the beam energy. Compare to the scintillator signal (less

ISBN 978-3-95450-178-6

Table 2: Summary of the beam distribution simulated, extension in real space are given in term of σ of the beam core type, the divergence can be seen in Fig. 3

	Extension	
Name	real space	divergence
"20sig."	20σ uniform	flat
"15sig. flat"	15σ uniform	flat
"15sig. gauss"	15σ gauss	gauss high
"10sig. flat"	10σ uniform	flat
"10sig. gauss"	10σ uniform	gauss high
"Nominal"	10σ flat	gauss low

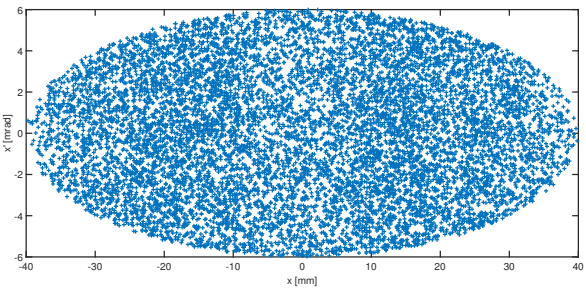

Figure 4: Distribution of the particles in the phase space for the "20sig." case (beam energy is 200 MeV) .

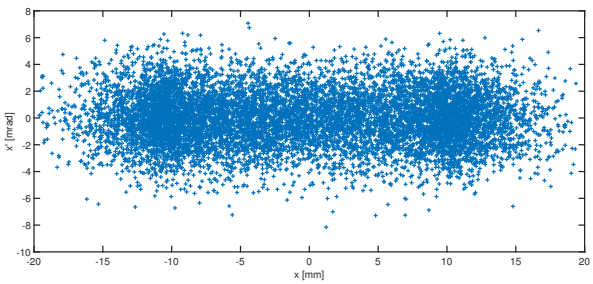

Figure 5: Distribution of the particles in the phase space for the "10sig. gauss" case (beam energy is 200 MeV).

than 1 keV per primary), in all the cases the beam loss signal on the detector will be much higher than the expected signal during a profile measurement.

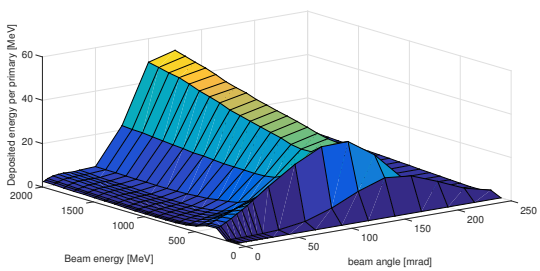

Figure 6: Estimated energy deposited in detector 1 as function of the beam energy and angle of impact. The loss is in middle of the upstream quadrupole.

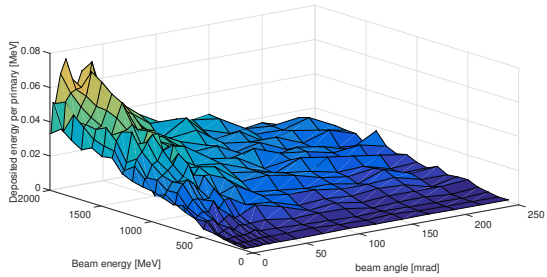

Figure 7: Estimated energy deposited in detector 1 as function of the beam energy and angle of impact. The loss is in middle of the downstream quadrupole.

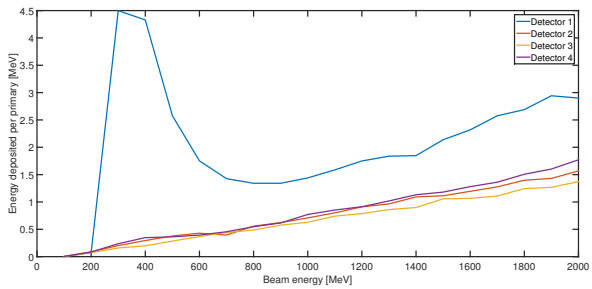

Figure 8: Evolution of the deposited energy as function of the beam energy on the 4 detectors, the beam impacts in the upstream quadrupole with an angle of 3 mrad.

From these results, it seems possible to detect the position of a losses, also detect the direction of the loss, a clear difference on the signal of each detector can be detected (see Fig. 8).

For the cases of unwanted beam steering, like the previous results, the WS acquisition will be fully saturated as shown in Figs. 9 and 10.

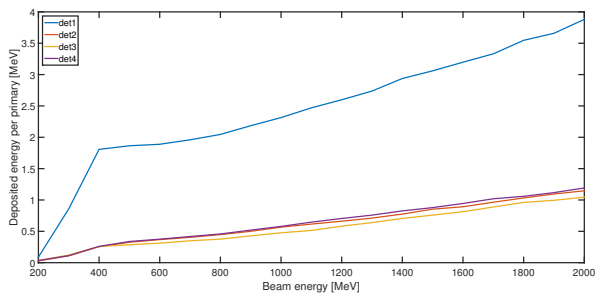

Figure 9: Evolution of the energy deposited in each scintillator as function of the beam energy, the impact is in the middle of the upstream quadrupole corresponding to an angular kick of 6 mrad.

For the 6 mrad case, it is interesting to note that the loss direction can be detected and the signal on the detector 1 increase rapidly below 400 MeV and slowly above and up to 2 GeV. This can be explain by the cinematic of the reaction ad the detector geometry, the signal on the scintillator is dominated by the energy deposition induced by protons.

ISBN 978-3-95450-178-6

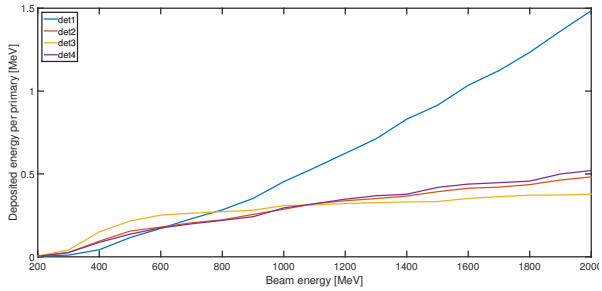

Figure 10: Evolution of the energy deposited in each scintillator as function of the beam energy, the impact is in the middle of the upstream cryomodule corresponding to an angular kick of 10 mrad.

Below 400 MeV, more than 80 % of the signal is generated by protons, above this energy, the protons are emitted in a cone which becomes smaller when the beam energy increases, as consequence a smaller portion of this particle interacts with the scintillator and their contribution to the signal decreases. Nevertheless, the production of secondaries particles increases with the energy and therefor increase the signal, at 2 GeV, 50 % of the signal is induced by the secondaries particles.

The signal on the other detectors increase almost linearly with the beam energy.

For a beam impacts in the middle of the cryomodule, at low energy the signal on all the detectors are more or less equal, the direction of the loss can be detected only at high energy. In this case, the beam and the product of the induced shower interact with more matter than in the previous case, due to this interaction, at low energy the flux of particles will be almost uniform at the scintillator location, while as the energy increases, the beam interacts less an less with the matter leading to a rapid increase of signal of the detector positioned in the same quadrant of the loss.

Halo

For a given distribution and a given beam energy, as shown in Fig. 11 the signal on the 4 detectors is almost identical, thus all the following results are presented for a single detector.

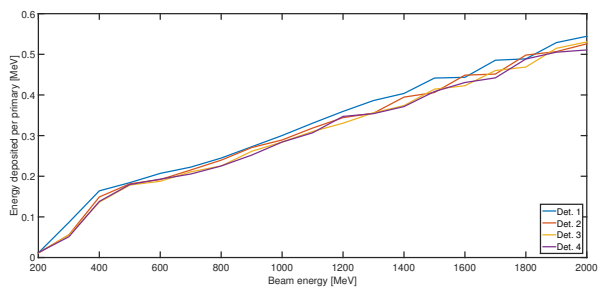

Figure 11: Evolution of the energy deposited in each scintillator as function of the beam energy, for the beam distribution "fil. uniform"

Energy deposition With the same particle distribution for the energies considered, the energy deposited in the detector increases with the beam energy (see Fig. 12). it also appears clearly that the beam divergence has a strong impact on the losses, more important than the extension in the real space.

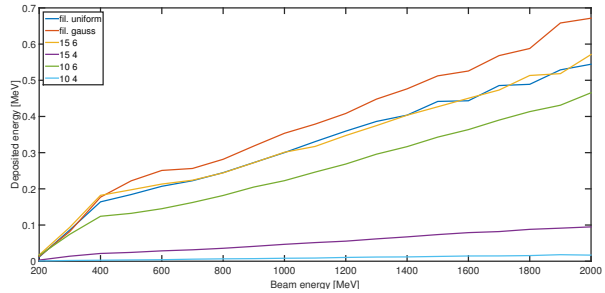

Figure 12: Evolution of the energy deposited in one scintillator as function of the beam energy, the distributions in this figure are independent of the beam energy.

The same influence of the beam halo divergence can be seen when the influence of the acceleration has been simulated (see Fig. 13).

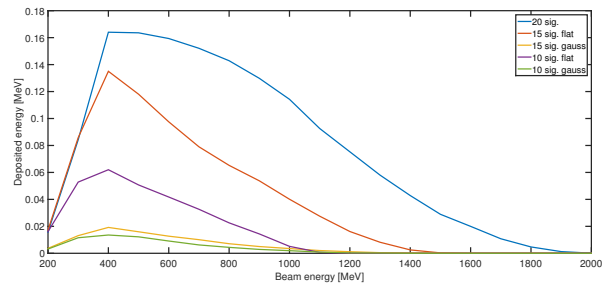

Figure 13: Evolution of the energy deposited in one scintillator as function of the beam energy, beam halo divergence is decreasing with the energy .

In all the cases, the peak energy deposition is around 400 MeV. Above this energy, the signal decreases with the beam energy, due to the smaller divergence, at the exception of the biggest beam the signal is almost zero above 1500 MeV, nevertheless due to the small statistic in the MC simulations and of the cut in the particle distribution, some losses are expected in the high energy range of the ESS linac, It appears that the losses might be an issue between 200 and 600 MeV, which corresponds to the ESS medium β section energy range. The influence of the beam divergence is important, with a lower divergence ("nominal" beam in Fig. 3) the energy deposited is almost null above 300 MeV.

Due to the simplified geometry and the low statistic present in the simulation, the peak at 400 MeV might be artifact of the MC simulations, depending on the amount of matter that the loss particles will see this peak might slightly move. These data are certainly not a representative of the losses expected in the ESS linac, nevertheless, they can be used to set the operating domain of the WS.

ISBN 978-3-95450-178-6

Signal The previous results were uses to estimate the Signal to Noise Ration (SNR) expected during a beam profile measurement. The expected peak signal from the WS as been simulated with the same geometry and assuming a 40 μm tungsten wire. The minimum signal is expected for a beam energy of 400 MeV, the maximum signal at 2000 MEV. In post processing and with the date presented in the previous section, the background signal has been estimated for various proportion of particles in the halo and the expected Signal to Noise Ration (SNR) during a beam profile measurement has been calculated for the lowest expected signal (400 MeV). The results are summarized in Figs. 14 and 15.

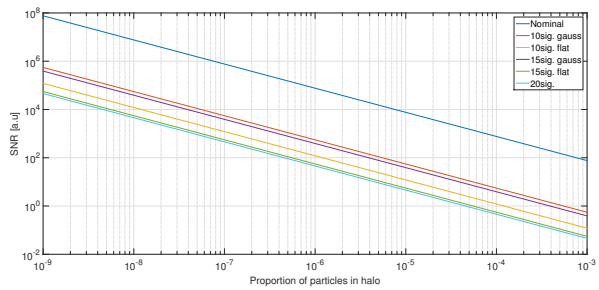

Figure 14: Expected SNR at 400 MeV for beam halo distribution independent of the beam energy.

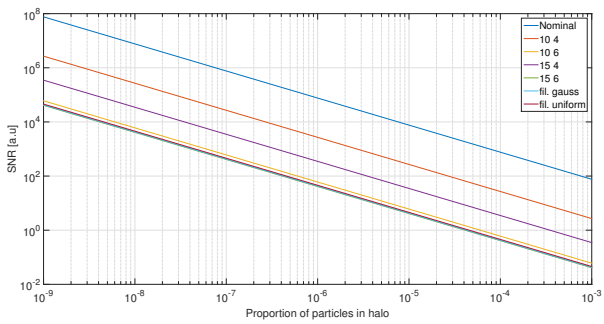

Figure 15: Expected SNR at 400 MeV for beam halo distribution dependent of the beam energy.

In all cases, if the 10^{-9} of the particles are in the halo as simulated in the MC code, the SNR is better than 10^4, if this proportion increase to 10^{-6} the SNR will be $\approx$ 100 in the worst case and up to 10^{-5} in the best case simulated. At High energy, for the cases with a divergence decreasing with the beam energy, the SNR increases. The reconstruction of the beam profile might be compromised if the losses in the ESS superconducting linac is too high.

CONCLUSION AND PERSPECTIVE

The studies presented in this paper might be far from what will be observed in the ESS linac, the low statistic in the MC simulations as well as the arbitrary beam distributions induced certainly large uncertainty on the results. Nevertheless, the two extreme cases presented in Figs. 14 and 15 are setting the limits for the expected beam losses.

These preliminary studies show that the WS detectors are quite sensitive to beam losses, the performance of the WS might suffer if the losses exceed 10^{-6} and if the halo is not mitigate.The detector concept proposed for the ESS wire scanner shows an interesting sensitivity to the beam halo parameters. In high power hadron linac, matching the halo seems a better alternative to the classical core matching in order to reduce the beam losses toe an acceptable level [5], the detector part of the WS system might be used not only to measure the beam core profile but also, together with other monitors like the Beam Loss Monitor [6], to match the beam halo.

In order to confirm the ability of the WS system to be used for the halo matching, the particles distributions used for the simulation must be refined with dedicated beam dynamic simulations. More accurate MC simulations are as well needed, in particular, the effect of losses over few period need to be simulated. The electromagnetic field of the quadrupoles and the cavities might affect the beam loss pattern, and therefore must be studied.

REFERENCES

[1] M. Eshraqi et al.,"The ESS linac", in *Proc. IPAC '14*, Dresden, Germany, THPME043.

[2] B. Cheymol, "Scintillator detectors for the ESS high energy wire scanner" in *Proc. HB'16*, Malmo, Sweden.

[3] A. Ferrari, P.R. Sala, A. Fasso, and J. Ranft, "FLUKA: a multi-particle transport code" CERN-2005-10 (2005), INFN/TC_05/11, SLAC-R-773.

[4] R. Miyamoto., "An ESS linac collimation study", in *Proc. HB'14*, East-Lansing, MI, USA.

[5] N. Chauvin et al., "Halo Matching for High Intensity Linacs and Dedicated Diagnostics", in *Proc. HB'14*, East-Lansing, MI, USA.

[6] I. Dolenc Kittelmann, "Simulations and Detector Technologies for the Beam Loss Monitoring System at the ESS Linac" in *Proc. HB'16*, Malmo, Sweden.

ISBN 978-3-95450-178-6